A Simple Technique to Generate In-Plane Forming Limit Curves and Selected Applications

K.S. RAGHAVAN

A simple technique to generate in-plane forming limit curves has been developed. This technique is based on the Marciniak biaxial stretch test using a single punch/die configuration, but the specimen and washer geometries have been modified in order to achieve failure in both drawing and stretching deformation modes. The experimental technique is described, and the advantages of using this in-plane method over the conventional out-of-plane dome method are discussed. It is shown that (a) sheet thickness has an intrinsic influence on forming limits that is not related to small bending strain variations with thickness or to deformation in the presence of friction and curvature, (b) plastic anisotropy ($\bar{r}$ value) does not substantially affect forming limits, and (c) in-plane forming limits are slightly lower (5 to 6 pct) than out-of-plane forming limits near plane strain; these differences are smaller than previously reported values (12 to 15 pct) in the literature.

I. INTRODUCTION

FORMING limit diagrams (FLDs), which compare the strains in an industrial stamping to the forming limit curve (FLC) for the sheet metal, are extensively used in the North American forming community (particularly automotive) for tooling trials prior to production stamping and for problem identification/resolution in the production environment.[1,2] The forming limit curve shown on a forming limit diagram represents limiting principal surface strains corresponding to the onset of localized necking for a wide range of strain paths.

The common approach used in North America to determine FLCs is the out-of-plane technique (Figure 1), which involves stretching different width specimens over a rigid punch following the method proposed by Hecker.[3] By varying the specimen width, the lateral constraint (*i.e.*, the amount of material allowed to draw into the die cavity in the width direction) can be varied to achieve failure in modes ranging from uniaxial tension through plane strain to balanced biaxial tension (Figure 2). Some characteristics of out-of-plane punch stretching include the following: (a) the deformation is constrained by tooling geometry, and failure is forced to occur at specific locations in the specimen; (b) bending strains are imposed on the sheet sample, the magnitude of which depend on sheet thickness and punch radius; and (c) large strain gradients are produced because of the presence of friction and curvature. Because of these characteristics, forming limits determined using the out-of-plane method show a dependence on tooling geometry variables such as punch radius.[4] Furthermore, because of the relatively large strain gradients in the specimen imposed by the geometric constraints, strain levels corresponding to failed (necked) and acceptable states are widely separated. Multiple specimens deformed to various fractions of failure height are often necessary to determine limit strains accurately with this method. Finally, because failure occurs in the test specimen at specific locations that are dictated by specimen and tooling geometry, the out-of-plane method is not very sensitive to material defects.

An alternate approach to determine forming limit curves is to use an in-plane method. In this case, deformation may be accomplished in a uniform and proportional manner (ϵ_2/ϵ_1 kept constant during straining) within the plane of the sheet sample, without imposing any bending on the specimen and avoiding friction effects. Because of these attributes, in-plane forming limits can be more sensitive to material defects and are not influenced to the same extent by tooling geometry variables. Furthermore, since curvature and friction effects are absent, large strain gradients can be avoided in the in-plane test, allowing forming limits to be more accurately defined. Despite these advantages, the in-plane approach is not widely used to develop forming limit curves, perhaps because of the lack of a good streamlined technique to determine forming limits in different strain paths. Although a few in-plane FLC methods have been developed in the past, most of these methods are restricted to determining forming limits in a limited number of strain paths. Azrin and Backofen[5] generated in-plane forming limits for proportional strain paths ranging from plane strain ($\rho = \epsilon_2/\epsilon_1 = 0$) to a biaxial stretch corresponding to $\rho = 0.6$. Their approach involved first producing a uniformly thinned elongated "patch" at the center of a much larger sheet (the thickness of the patched region was effectively half that of the parent sheet). The sheet containing the patch was gridded and stretched over a large radius hemispherical punch until localized necking occurred in the patched region. The eccentricity of the patch was varied to generate failure at strain states from $\rho = 0$ to 0.6. Marciniak and Kuczynski[6] developed an ingenious technique to deform sheet specimens in-plane under balanced-biaxial conditions. In this approach, a flat punch with circular cross section is used to deform the specimen, not directly but through a second blank (washer) having a central hole. Although the specimen and the washer are deformed out of plane by the flat punch, the region of interest in the specimen which is in "contact" with the hole in the washer deforms effectively under in-plane stretching conditions. Tadros and Mellor[7] modified the Marciniak technique by varying

K.S. RAGHAVAN, Research Engineer, is with the Cold Rolled and Coated Sheet Division, Bethlehem Steel Corporation, Bethlehem, PA 18016-7699.

Manuscript submitted August 4, 1994.

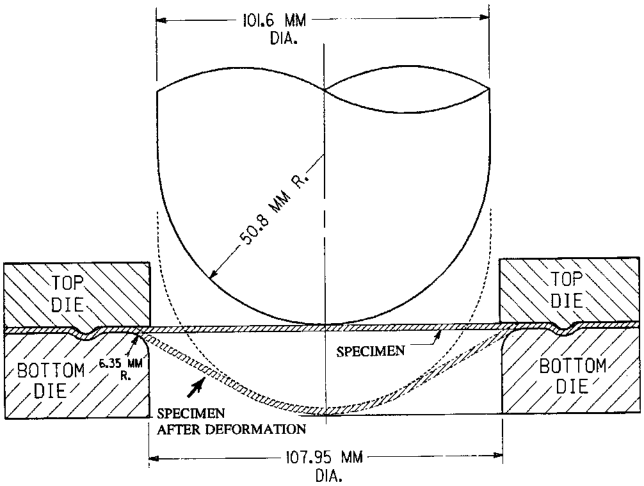

Fig. 1—Schematic diagram showing the tooling geometry used in the out-of-plane FLC test. Note curvature taken on by the specimen after deformation.

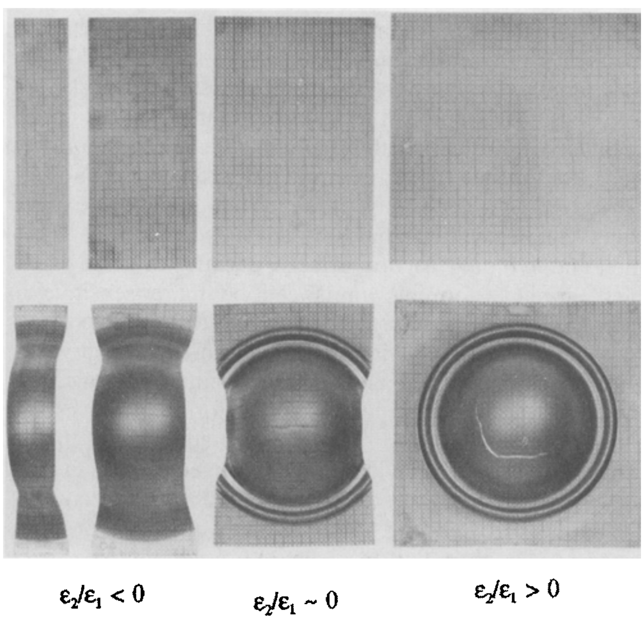

Fig. 2—Typical specimens before and after deformation in the out-of-plane FLC test which were used to determine forming limits in drawing ($\epsilon_2/\epsilon_1 < 0$) and stretching ($\epsilon_2/\epsilon_1 > 0$) conditions.

punch ellipticity to achieve failure in a few strain states ranging from plane strain to balanced-biaxial stretching. Gronostajski and Dolny[8] have also used the Marciniak approach to generate FLCs by modifying specimen and washer geometries.

In this article, a simple technique to generate in-plane forming limits is described. The in-plane technique discussed here is similar to that of Gronostajski and Dolny[8] but differs in the choice of specimens and washers used to generate the FLC. Unlike the earlier in-plane approaches, forming limits can be determined over a wide range of strain paths using the method discussed here. The experimental technique is described, and the advantage of using this in-plane method over the out-of-plane dome method is demonstrated *via* two applications, *i.e.*, studying the effects of sheet thickness and plastic anisotropy on forming limits. Comparisons between in-plane and out-of-plane forming limits are also made in the article and are discussed in the context of previous work.

II. DESCRIPTION OF IN-PLANE FLC TEST METHOD

A schematic diagram showing the Marciniak test setup is shown in Figure 3. A flat punch drives the test specimen indirectly through a washer with a central hole. As the punch descends, the hole in the washer expands radially. Radial friction forces appear in the contact region between the test piece and the washer. This friction prevents the test piece from fracturing near the rounded edge of the punch, and the largest strains are found in the flat central part of the specimen. For a fully constrained test specimen, the area of interest which is in contact with the hole in the washer, deformation is uniformly balanced-biaxial and occurs under frictionless conditions, allowing instability and failure to occur anywhere in this region.

While the Marciniak technique has commonly been used to study the role of material defects under balanced-biaxial stretching conditions, we have modified the specimen and washer geometries in order to achieve failures in different strain states ranging from uniaxial to balanced-biaxial tension. For convenience, we have categorized the specimens

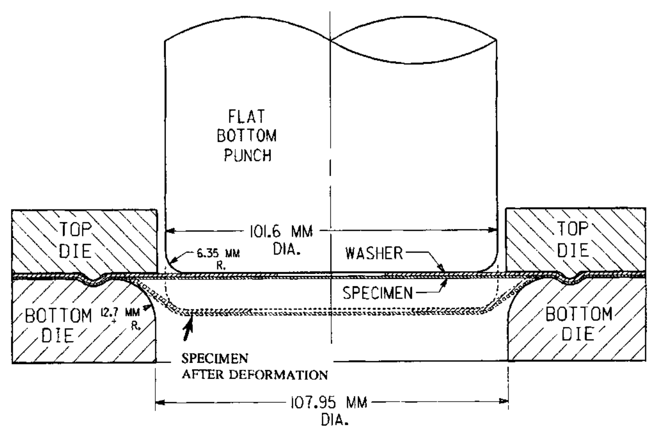

Fig. 3—Schematic diagram showing tooling geometry used in the in-plane FLC test. Note that the specimen region of interest remains planar during testing (compare to Fig. 1 which shows typical specimens deformed out of plane.)

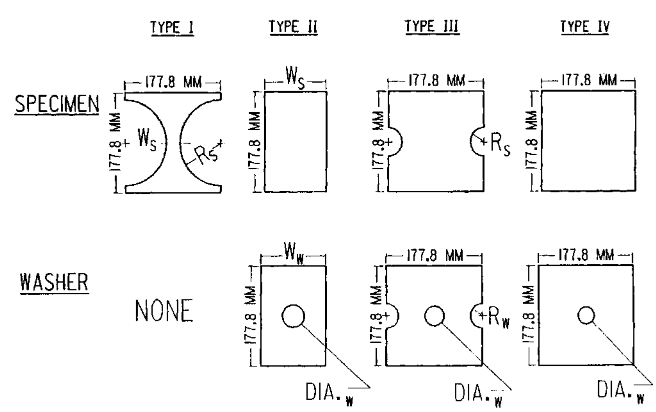

Fig. 4—Typical specimen (top) and washer (bottom) configurations used to generate failure corresponding to different drawing and stretching strain states in the in-plane FLC test.

Table I. Specimen and Washer Geometries Used to Determine In-Plane Forming Limits for Low-Carbon Sheet Steel

Specimen Type	Effective Specimen Width, W_s (mm)	Notch Radius R_s (mm)	Washer Hole Diameter W_d (mm)	Minor Strain Range at Failure (Pct)
Type I (notched specimens)	25.4	76.2	no washer used	−25 to − 10 pct
	38.1	69.85		
	50.8	63.5		
	63.5	57.15		
	76.2	50.8		
Type II (parallel sided specimens/washers)	101.60	no notch	40.64	−10 to + 10 pct
	107.90		40.64	
	114.25		40.64	
	120.60		40.64	
	126.95		40.64	
	133.35		38.1	
	139.70		38.1	
Type III (notched specimens/washers)	120.65	28.575	40.64	+15 to +40 pct
	127.00	25.4	38.1	
	133.5	22.15	38.1	
	139.7	19.05	35.56	
Type IV (177.8-mm square specimen/washer)	177.8	no notch	30.5	balanced-biaxial (> +40 pct)

Note: length dimension = 177.8 mm for all specimen types. (Fractional dimensions appear in the table because of the use of metric units. Specimen/Washer dimensions can be better appreciated by converting to English units, 1 in. = 25.4 mm.)

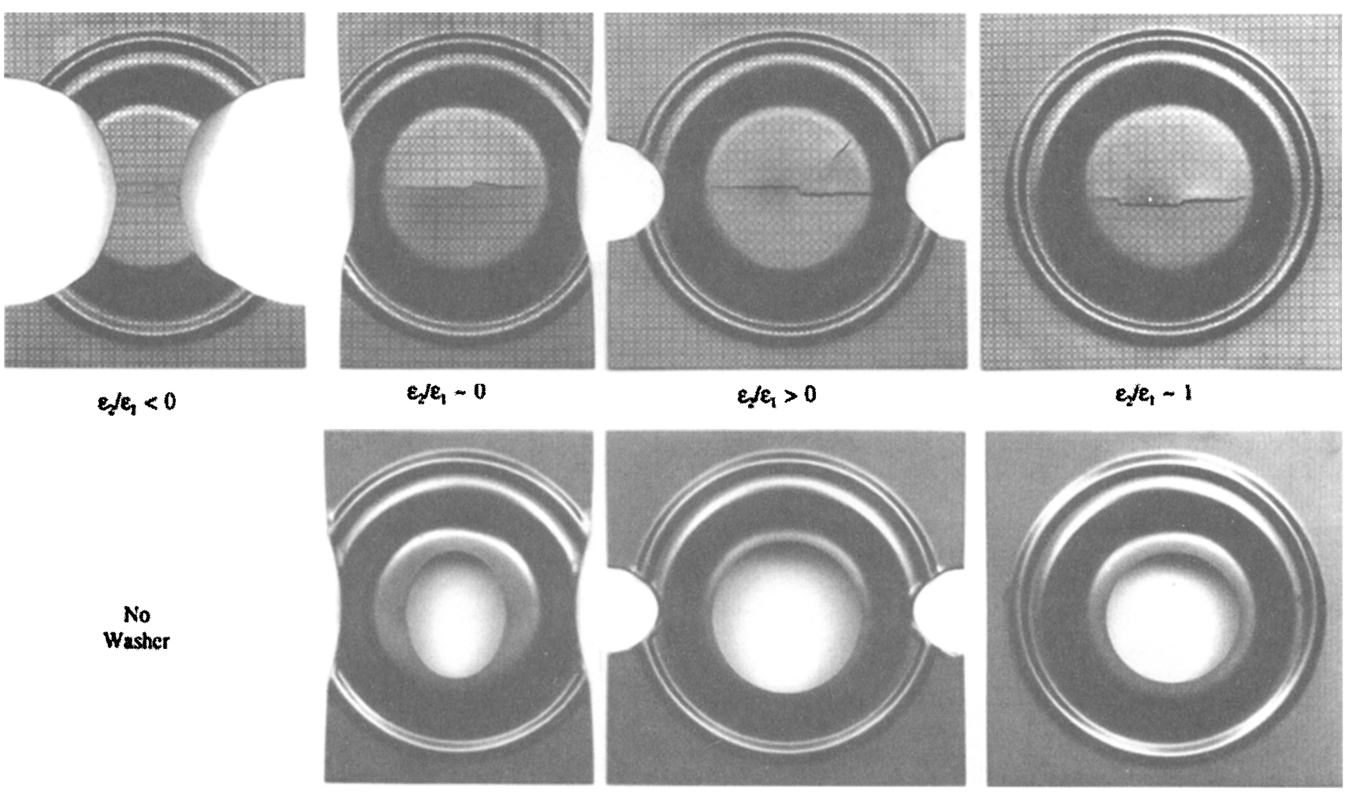

Fig. 5—Tested in-plane FLC specimens and corresponding washers showing failure in different strain states. (Note that the deformed area of interest remains planar during the test.)

used into four types (Figure 4 and Table I detail further information on the actual specimen and washer geometries used to determine forming limits for low-carbon sheet steels). Specimens of type I were used to determine forming limits in the draw region (negative minor strains ranging from $e_2 = -25$ to -10 pct). No washers were used with these specimens, and the localization process is similar to what is observed in the sheet tensile test. Specimens of type II were used to determine forming limits near plane strain (e_2 ranging from -10 to $+10$ pct). The geometry of the specimens (relatively wide and parallel sided) constrains deformation in the width direction, resulting in failures oc-

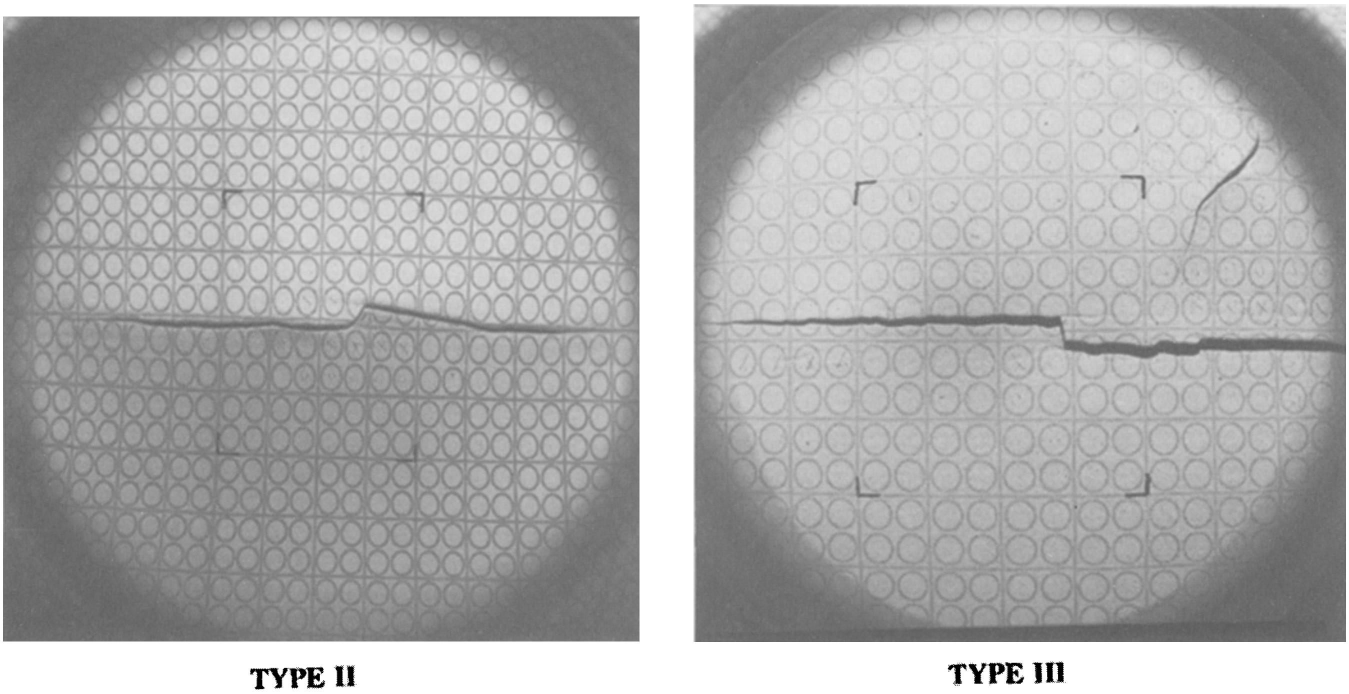

Fig. 6—Typical type II and III specimens showing deformation pattern and multiple necking occurrence in the specimen area of interest. (Bracketed region represents the deformed shape of a 1 × 1 in. area in the undeformed configuration.)

curring near plane strain conditions. Specimens of types III and IV were used to determine forming limits under stretching conditions. Specimen type IV has been used commonly for the classical Marciniak balanced-biaxial test, while specimens of type III are slightly notched to relax lateral constraints and allow failure to occur in stretching states with e_2 ranging from +15 pct to +40 pct.

Figure 5 shows typical specimens and corresponding washers of the four different types after in-plane deformation. Notice that the washer hole deformed differently depending on specimen type, and the selection of appropriate washer hole diameter (Table I) was critical to the success of the test. Figure 6 shows the typical deformed type II and III specimens at higher magnification in order to reveal the strain distributions more clearly and to indicate the presence of multiple necks. For the fully constrained classical Marciniak (type IV) specimen, it is well recognized[6,7,8] that the strain distribution in the specimen area of interest is uniformly balanced-biaxial tension. Failure can initiate anywhere in this region, resulting typically in several necked states near balanced-biaxial stretching conditions. For the remaining specimens (types I, through III), the strain distribution is not as uniform, and failure tends to occur close to the center of the specimen. Although the geometry of the specimen constrains failure to occur near the center, notice that the fracture path is not entirely straight for either the type II or III specimen in Figure 6, suggesting that some defect sensitivity is retained even for non-balanced-biaxial conditions. (In the out-of-plane dome samples, additional constraint is imposed on the failure location because of tooling curvature.) Principal major and minor strain distributions corresponding to a 1 × 1 in. specimen area in the undeformed configuration are presented for the typical type II and III specimens in Figure 7. (The deformed geometry of the original 1 × 1 in. area is shown enclosed by brackets in Figure 6.) While the major strain measurements for the type II specimen (Figure 7(a)) reveal a clear strain gradient (minor strain being uniformly near $e_2 = 0$), the difference between "necked" and "safe" strain states was quite small (~3 to 5 pct), allowing forming limits to be accurately defined. For the type III specimen, the major strain distribution appears to be quite uniform, but the minor strain shows a gradient particularly in the specimen width direction (Figure 7(b)); this latter feature allowed multiple necks with varying degrees of biaxiality to be formed across the specimen width. Type I specimens, particularly those used for determining forming limits in the large negative minor strain regime, exhibit pronounced strain gradients, similar to what one encounters in uniaxial sheet tensile specimens. Overall, because of the multiple necking occurrence and the relatively small strain gradients, our experience indicated that this in-plane method required fewer specimens to accurately define the forming limits compared to the conventional out-of-plane dome method. Furthermore, since the specimens remained flat after in-plane deformation, strain measurements were easier to perform than on curved panels associated with the out-of-plane dome method.

Tests to determine the in-plane forming limit curves of sheet steel were conducted on a laboratory press with a punch force capacity of 1350 KN. Sufficient clamp force (approximately 500 KN) was used to prevent draw-in of the sheet metal from the blankholder area. Tests were conducted at a punch displacement rate of 4.2 mm/s and were stopped at or just prior to specimen fracture in order to capture the onset of localized necking. Figure 8 shows a typical forming limit curve developed using the in-plane technique for a 0.76-mm low-carbon drawing quality sheet steel sample. The specimen and washer combinations used to achieve limiting (*i.e.*, localized necking) states in different strain paths are indicated in the figure.

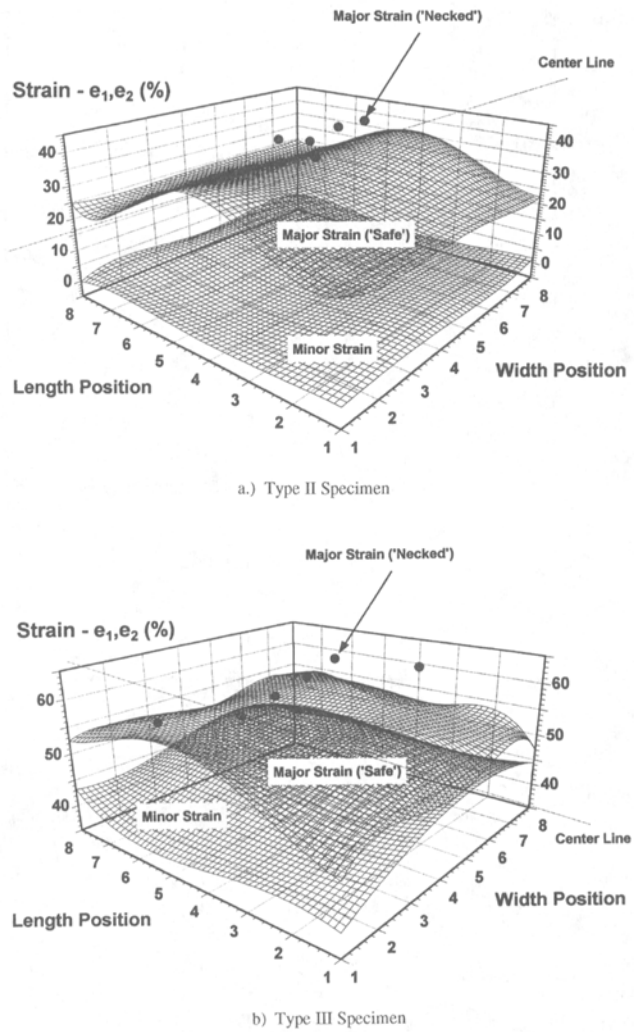

Fig. 7—Major and minor strain distributions corresponding to a 1 × 1 in. area in the undeformed configuration for the typical type II and III specimens (see Fig. 6 for location over which strains were measured).

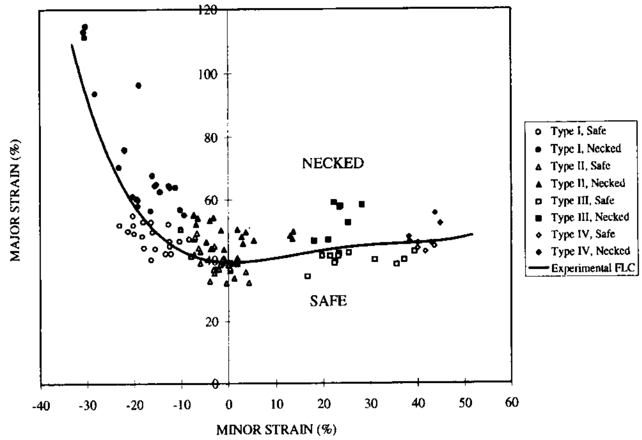

Fig. 8—Typical in-plane FLC for 0.76-mm-thick low-carbon drawing quality sheet steel. (Specimen types used to generate failure in different strain paths are also indicated in the figure.)

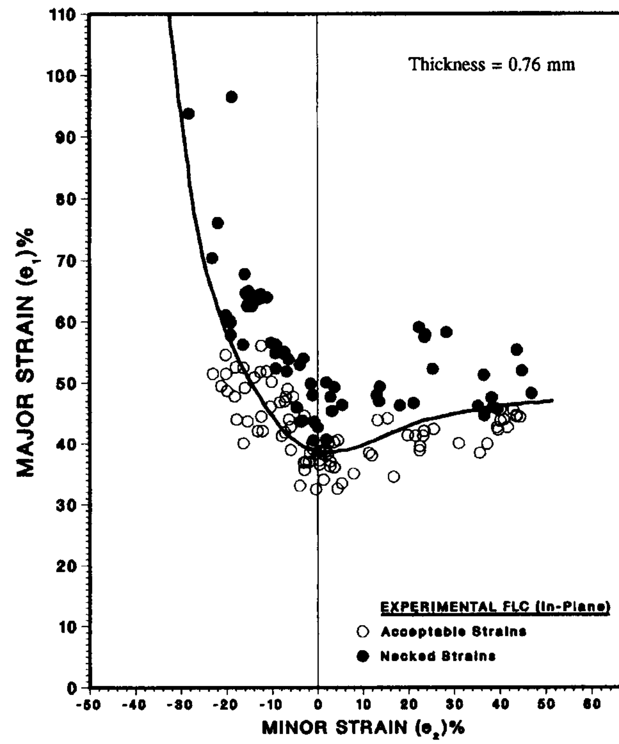

Fig. 9—In-plane FLC for 0.76-mm-thick low-carbon drawing quality sheet steel.

III. SELECTED APPLICATIONS OF THE IN-PLANE TECHNIQUE

A. *Influence of Sheet Thickness on Forming Limits*

It is commonly believed that the thickness of sheet metal has a strong influence on its formability. Work done by Keeler[9] and Lee and Hiam[10] suggests that thicker sheets have higher forming limits, and a nomogram developed by Keeler and Brazier[11] is widely used in North America to predict forming limits as a function of sheet thickness. Different theoretical explanations have been proposed to account for the observed thickness dependence of forming limits.[12–15] Hutchinson *et al.*[12] suggest that the increase in forming limits with thickness is due to the development of triaxial stresses in the localized neck which increase with increasing sheet thickness. Rao and Chaturvedi[13] used a Bridgeman type analysis to account for triaxial stresses within a Marciniak–Kuczynski (MK) analysis[6] and showed that the predicted forming limits increase with sheet thickness. Gotoh *et al.*,[14] using a vertex type yield formulation, performed bifurcation analysis to determine forming limits under balanced-biaxial stretching. They also predicted that the critical strain corresponding to localized necking increases with sheet thickness. Schmitt and Jalinier[15] offer a different explanation for the observed increase in forming limits with thickness, suggesting that void growth is faster in thinner sheets resulting in the occurrence of localized necking at lower strain levels for thinner sheets.

Doubts have persisted, however, as to the existence of an intrinsic effect of thickness on forming limits. These doubts stem from the fact that the observed thickness dependence is generally based on forming limits determined by stretching sheets over a rigid hemispherical punch (out of plane). In these tests, the bending strains imposed on the sheet increase with sheet thickness,[16] and the change in bending strains is claimed to account, at least in part, for the experimentally observed thickness effect. Triantafyllidis and Samanta[17] have examined the effects of sheet thick-

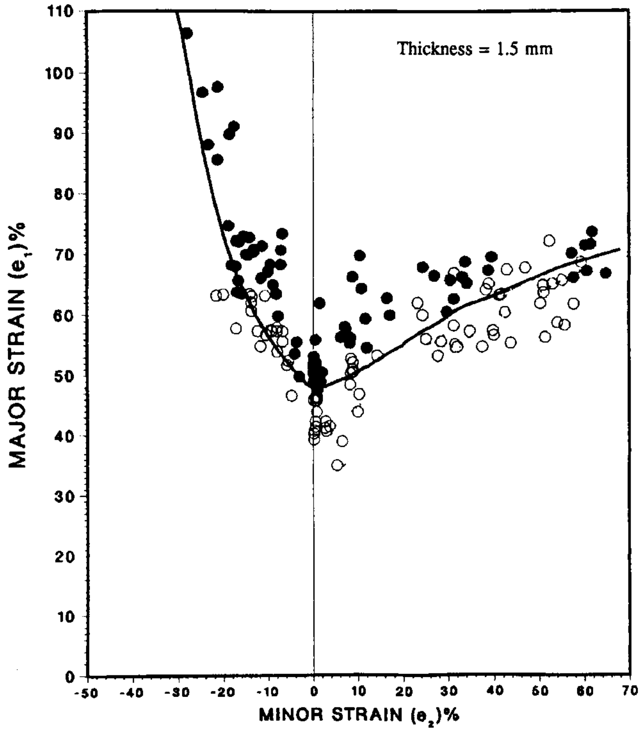

Fig. 10—In-plane FLC for 1.5-mm-thick low-carbon drawing quality sheet steel.

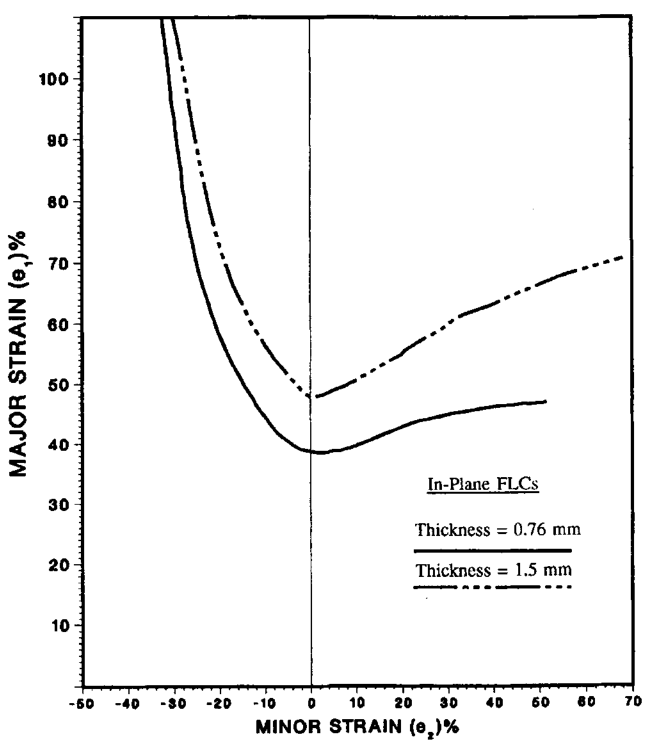

Fig. 11—Comparison of in-plane FLCs showing a substantial effect of sheet thickness (~10 pct) on forming limits.

ness and curvature on flow localization using a three-dimensional finite element model based on a nonlinear shell theory[18] which fully accounts for bending effects. They conclude, based on experimental and numerical calculations, that if the onset of strain localization is used as the failure criterion, material thickness has little influence, while the observed thickness dependence of forming limits

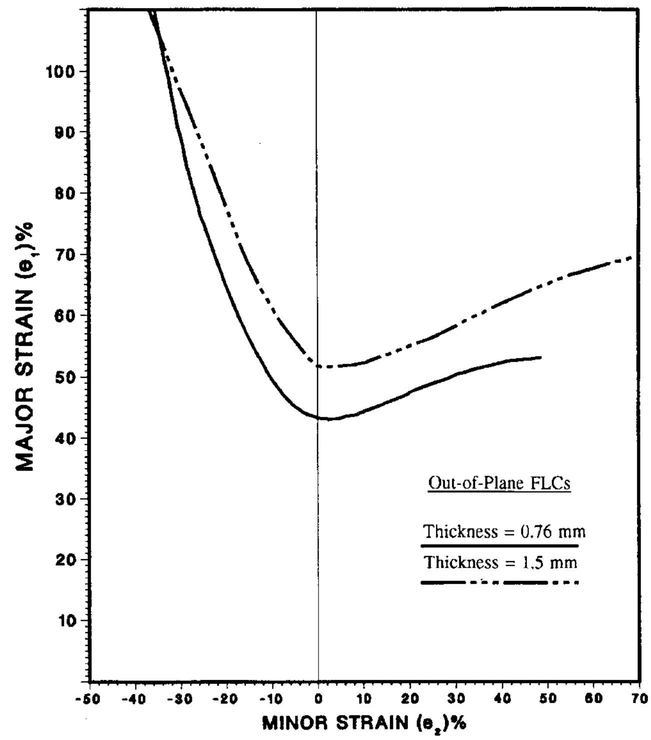

Fig. 12—Comparison of out-of-plane FLCs showing substantial effect of sheet thickness on forming limits. Notice the similar magnitude in the difference between the 0.76- and 1.5-mm-thick sheet forming limits under in-plane and out-of-plane conditions (compare Figs. 11 and 12).

arises because of differences in the growth of localized necks in thin and thick sheets. For thin sheets, they predict that there is no significant difference between the strain corresponding to onset of localization and the fracture strain. For thick sheets, however, Triantafyllidis and Samanta[17] predict that strain localization does not proceed rapidly after the onset of localization. They argue, therefore, that the common experimental practice of determining forming limits close to failure rather than at the onset of localization results in increased forming limits with sheet thickness. Another explanation suggesting that the thickness effect is not intrinsic has been proposed by Hosford.[19] Assuming geometrically similar necks in thin and thick sheets, it is argued that the localized neck is wider in thicker sheets compared to thin sheets. Since the same grid size (usually 2.54 mm) is used to determine forming limits regardless of thickness, it is claimed that the wider localized neck results in higher measured forming limits in thicker sheets.

Some of the difficulties associated with interpreting thickness effects in out-of-plane tests can be eliminated by using an in-plane technique. Since there is no curvature, there is no need to consider differences in forming limits arising from differences in bending strains with varying sheet thickness. While the argument suggesting that forming limits increase with thickness because of experimental measurement errors is still applicable, this effect is expected to be much less significant for in-plane deformation. Since the deformation is nominally uniform in the region of interest, the overall strain gradients are small, and relatively small differences (typically 3 to 5 strain percent) are seen between strained ellipses that show localized necks compared with those that show no localized necks. Thus, the

Table II. Chemical Compositions of Low-Carbon Steels Used to Study Thickness Effects

Material	C	Mn	P	S	Si	Al	N	O	Ti	Nb	B
Thickness = 0.76 mm	0.040	0.19	0.013	0.008	0.014	0.039	0.005	0.0037	<0.002	<0.005	<0.001
Thickness = 1.5 mm	0.053	0.25	0.009	0.007	0.010	0.056	0.005	0.0022	<0.002	<0.005	<0.001

Table III. Tensile Properties of Low-Carbon Steel Samples Used to Study Thickness Effects

Material Property	Yield Strength (Mpa)	Tensile Strength (Mpa)	Total Elongation (Pct)	*n* Value	$\bar{r}$ Value	Δr
Thickness = 0.76 mm	173	308	43.0	0.23	1.62	0.55
Thickness = 1.5 mm	168	317	43.0	0.23	1.55	0.64

Table IV. Chemical Compositions of Low-Carbon and IF Steel Samples Used to Study Plastic Anisotropy Effects

Material	C	Mn	P	S	Si	Al	N	O	Ti	Nb	B
Low carbon	0.039	0.20	0.012	0.008	0.010	0.056	0.005	0.0027	<0.002	<0.005	<0.001
IF	0.003	0.063	0.012	0.006	<0.010	0.049	0.005	0.003	0.034	0.050	<0.001

Table V. Tensile Properties of Low-Carbon and IF Steel Samples Used to Study Plastic Anisotropy Effects

Material Property	Yield Strength (Mpa)	Tensile Strength (Mpa)	Total Elongation (Pct)	*n* Value	$\bar{r}$ Value	Δr
Low carbon	169	314	43.5	0.263	1.24	0.41
IF	170	333	40.0	0.260	1.84	0.10

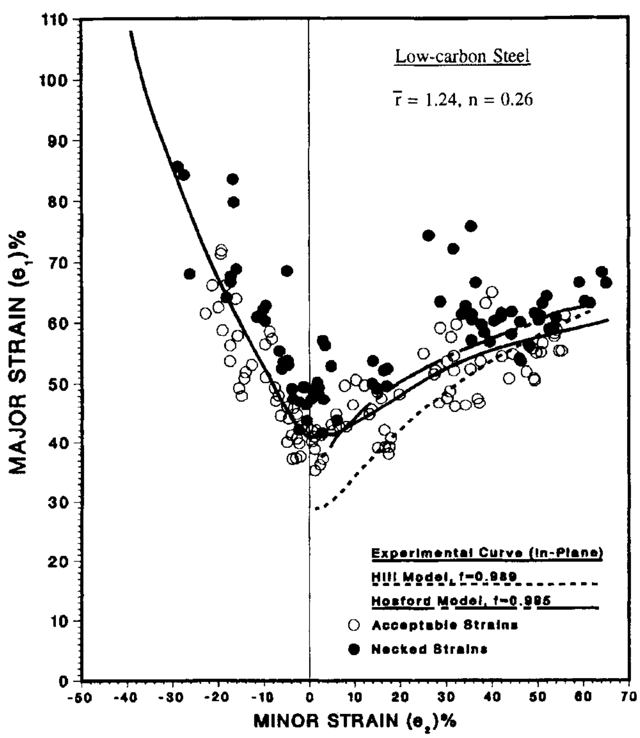

Fig. 13—In-plane FLC for low-carbon drawing quality steel with low $\bar{r}$ value.

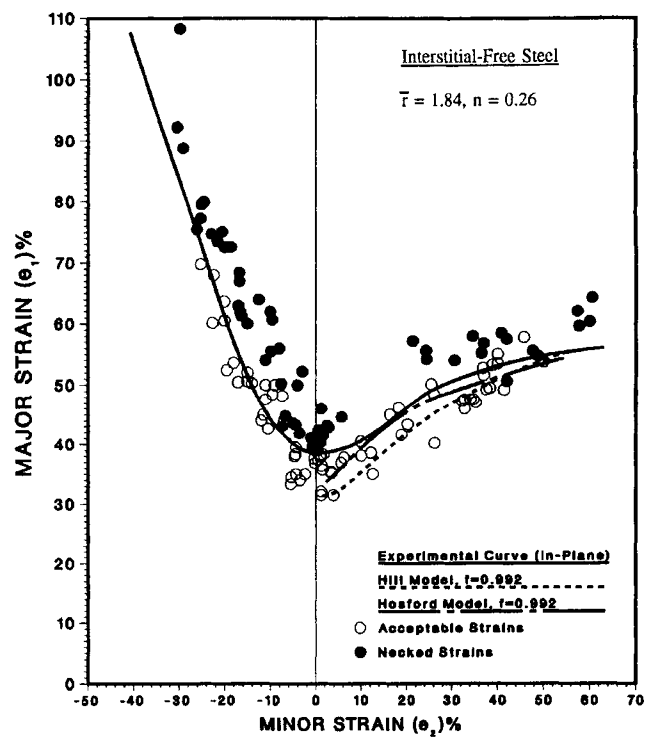

Fig. 14—In-plane FLC for IF steel with high $\bar{r}$ value.

change in forming limits with thickness because of differences in localized neck width or because of differences in the growth rate of localized necks would be restricted to about 3 to 5 pct, which is within the error involved in experimental forming limit determinations.

In-plane forming limit curves are shown in Figures 9 and 10 for low-carbon drawing quality cold-rolled steel with two different thicknesses (nominally 0.76 and 1.5 mm), and the differences are presented in Figure 11. (The chemistry and mechanical properties of the steels examined are very

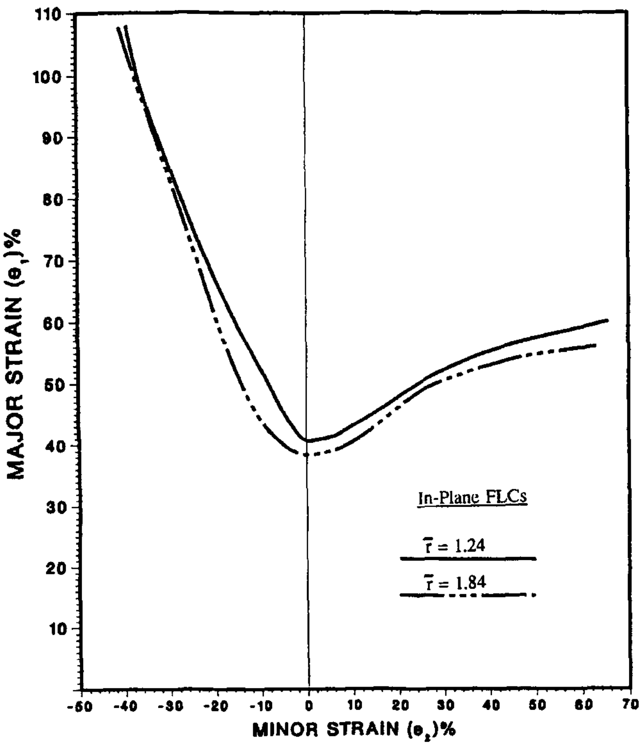

Fig. 15—Comparison of in-plane FLCs showing relatively small effect of $\bar{r}$ value on forming limits.

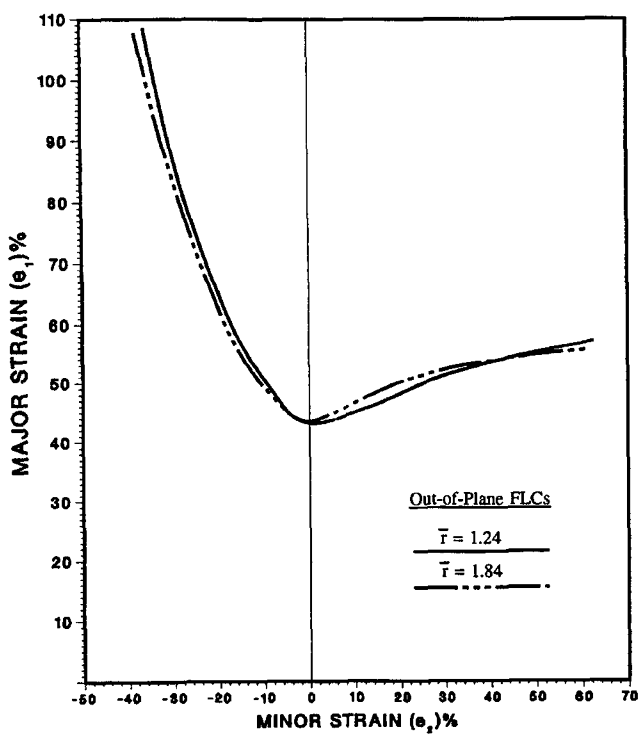

Fig. 16—Comparison of out-of-plane FLCs showing small effect of $\bar{r}$ value similar to the in-plane results in Fig. 15.

similar, as shown in Tables II and III, respectively.) Figure 11 clearly shows that in-plane forming limits increase substantially with thickness. For comparison, the influence of thickness on out-of-plane forming limits is shown in Figure 12. The magnitude of the thickness dependence of forming limits is quite similar in both cases (~10 pct strain for a

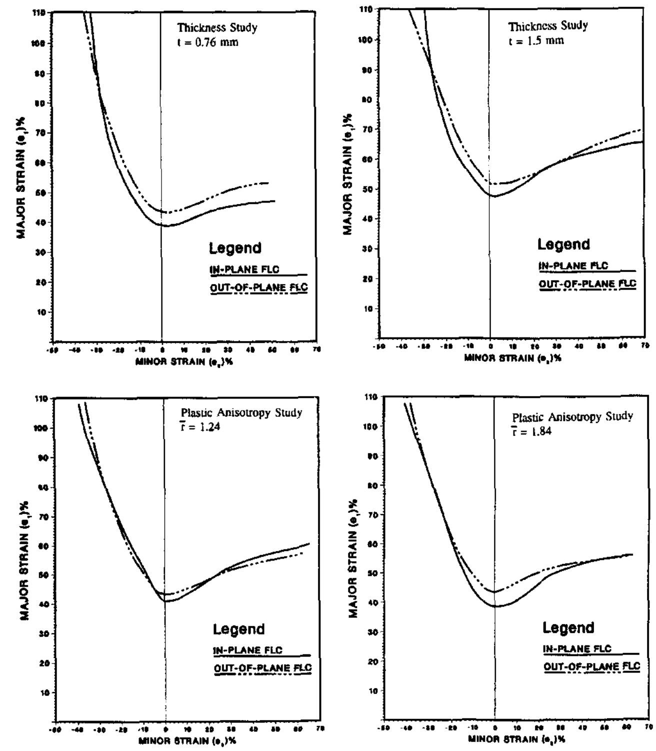

Fig. 17—Comparison of in-plane *vs* out-of-plane FLCs for sheet steels used in the thickness and plastic anisotropy studies. Note the relatively small difference between in-plane and out-of-plane forming limits (compare to Figure 18).

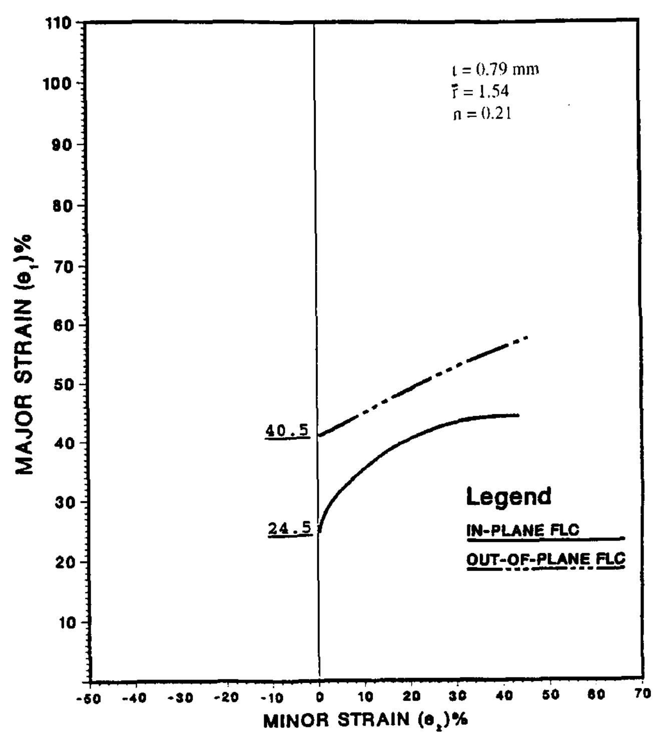

Fig. 18—Difference between in-plane and out-of-plane FLCs seen in the work of Ghosh and Hecker[25] for low-carbon aluminum-killed sheet steel. (Figure is author redrawn from original data in Fig. 3 of Reference 25 and replotted in terms of engineering strains to facilitate comparison to Fig. 17.)

0.74 mm increase in thickness), suggesting that simple bending strain changes with thickness, or deformation in the presence of friction and curvature, may not substantially influence the relationship between sheet thickness and forming limits.

B. *Influence of Plastic Anisotropy ($\bar{r}$ value) on Stretch Forming Limits*

Plastic anisotropy arises due to the preferred orientation of grains in a polycrystalline material and is usually characterized by the $\bar{r}$ value, a weighted average measure of the width-strain to thickness-strain ratio in tensile tests conducted along the longitudinal, transverse, and diagonal directions. It is generally recognized that a high $\bar{r}$ value is useful for improved drawability, but in stretch forming operations, the role of plastic anisotropy is less clear. Theoretical predictions of the effect of $\bar{r}$ value on stretch forming limits are conflicting, and experimental forming limit data explicitly comparing materials with change in $\bar{r}$ value but with other constitutive parameters held constant are not available. Most of the theoretical forming limit predictions reported in the literature use the MK approach,[6,20] which assumes that localized necking initiates from a pre-existing material imperfection under biaxial stretching conditions. While the imperfection may be metallurgical or geometrical in nature, it is commonly represented as a linear infinite groove normal to the largest principal straining direction. The MK analysis essentially assumes in-plane deformation conditions, and the magnitude, f, of the imperfection is used as an "adjustable" parameter selected to get a best fit to experimental data at plane strain or at balanced-biaxial tension. Theoretically calculated forming limits using the MK approach suggest that the form of the yield criterion (a scalar function which defines all stress combinations that would cause plastic yielding to occur) has a significant bearing on the predicted effect of stretch forming limits. For example, using the classical Hill[21] yield criterion, the MK analysis predicts a significant decrease in stretch forming limits with increasing $\bar{r}$ value, whereas no influence of $\bar{r}$ value on stretching limits is predicted when using the Hosford[22,23] yield criterion.

The in-plane test method was invaluable to study the effect of $\bar{r}$ value on forming limits, because it allowed direct comparison of experimental results to theoretical predictions based on MK models which implicitly assume in-plane deformation conditions. For the experimental work, materials were carefully selected to have a substantial variation in $\bar{r}$ value but with little change in other material constitutive parameters. The chemistry and properties of the materials used in this program are given in Tables IV and V, respectively. The low $\bar{r}$-value material was a low-carbon aluminum-killed chemistry specially processed using a high coiling temperature. The high $\bar{r}$-value material used was an interstitial free (IF) steel, with an n value equivalent to that of the low $\bar{r}$-value steel.

Experimental in-plane forming limits for the low-carbon and IF steel samples having different $\bar{r}$ values are shown in Figures 13 and 14 and compared together in Figure 15. Forming limit predictions based on the MK analysis using the classical Hill[21] and the Hosford[22] yield criteria are also shown with the experimental in-plane FLCs. Details of the specific MK analysis used to predict forming limits in this work are provided elsewhere.[24] The defect parameter, f, was chosen as the best fit to experimental data near balanced-biaxial stretching for all cases. For reference, the corresponding difference in out-of-plane forming limits tests is presented in Figure 16. It is quite clear from these results that the $\bar{r}$ value does not influence either the in-plane or out-of-plane forming limits (Figures 15 and 16) in a measurable way. This suggests the validity of yield criteria (such as Hosford's) which do not predict substantial changes in stretch forming limits with $\bar{r}$ values. However, it should be noted that the agreement between experimental data and theoretical predictions based on the MK analysis is not particularly good for either the Hill or the Hosford yield criteria (Figures 13 and 14), presumably because of the assumptions used in the MK analysis. Caution should therefore be exercised in relying on MK analyses to predict forming limits, and experimental FLC determinations remain necessary.[24]

C. *In-Plane vs Out-of-Plane Forming Limits*

It is widely believed that forming limits under constrained deformation conditions as experienced in out-of-plane tests are substantially higher than those determined under in-plane conditions. Under in-plane stretching conditions, localized necking is believed to occur at material-defect sites as assumed in the MK formulation[6,20] used commonly to predict forming limits. Under out-of-plane stretching conditions, however, Ghosh and Hecker[25] suggest that geometric constraints imposed by the tooling delay the strain localization process, resulting in substantially higher forming limits compared to in-plane limits.

In-plane and out-of-plane forming limits are compared for some of the sample materials used in the thickness and $\bar{r}$ value studies in Figure 17. Surprisingly, the difference between in-plane and out-of-plane forming limits was consistently quite small ($\sim$5 to 6 pct) compared to the results of Ghosh and Hecker[25] for low-carbon steel in Figure 18. (The original data presented in Figure 3 of Reference 25 was in terms of *true* strains and included results for brass and aluminum as well as low-carbon steel. To provide a good basis for comparison with the present work, the original data for low-carbon steel were replotted in terms of *engineering* strains in Figure 18.) The larger difference (12 to 15 pct) between in-plane and out-of-plane forming limits observed in the earlier work[25] may have arisen from the in-plane technique used in their study. To determine in-plane forming limits, Ghosh and Hecker[25] utilized Azrin and Backofen's procedure[5] in which the material tested in plane was effectively only half the thickness of the material used for determining out-of-plane limits. Considering that our results indicate a substantial influence of sheet thickness on forming limits, it is possible that the larger difference between in-plane and out-of-plane limits found in the earlier work[25] was influenced in part by thickness effects.

The relatively small difference (5 to 6 pct) between in-plane and out-of-plane forming limits seen in this work has important implications from an applications standpoint. Since production stampings experience varying degrees of in-plane or out-of-plane deformation (depending on part and tooling geometry), our results validate the current practice of using a single FLC to represent a material's forming capability in regions of complex stampings which encounter different deformation conditions. It must be noted, however, that for multistage deformation, the concept of using a single

FLC requires further examination because of the possible influence of strain path changes on forming limits.[26]

IV. SUMMARY

A simple technique to generate in-plane forming limit curves has been developed. This method is based on the Marciniak test, with the specimen/washer geometries modified to generate instability/failure in strain modes ranging from uniaxial tension through plane strain to balanced-biaxial stretching. The primary advantages of this technique over other in-plane techniques are the use of a single punch/die configuration to generate the entire FLC, the simple geometries of the specimens and washers used, and the overall ability to generate instability/failure in all strain paths from uniaxial tension to balanced-biaxial stretching. This method, like other in-plane test methods, is sensitive to material defects, imposes no bending strains on the sheet, allows relatively small strain gradients on the test specimen, and is characterized by nearly proportional loading paths. The usefulness of the in-plane method to examine the effects of sheet thickness and plastic anisotropy on forming limits is demonstrated in this article. It is shown that (a) sheet thickness has an intrinsic influence on forming limits, (b) plastic anisotropy ($\bar{r}$ value) does not substantially affect forming limits, and (c) in-plane forming limits are slightly lower (5 to 6 pct) than out-of-plane forming limits near plane strain; these differences are smaller than values (12 to 15 pct) previously reported in the literature.

ACKNOWLEDGMENTS

The author would like to acknowledge J.G. Speer for critically reviewing the manuscript. Substantial contributions made by R.C. VanKuren in developing the tooling to conduct the Marciniak test are acknowledged. Excellent technical support was provided by J.F. Layland, A.J. Sfarra, and H.L. Held throughout the course of this study. V. Jagannathan assisted with the preparation of the three-dimensional surface strain plots.

REFERENCES

1. S.P. Keeler: SAE Technical Paper No. 650545, 1965.
2. S.P. Keeler: SAE Technical Paper No. 680092, 1968.
3. S.S. Hecker: *Sheet Met. Ind.*, 1975, vol. 52, pp. 671-75.
4. P.L. Charpentier: *Metall. Trans. A*, 1975, vol. 6A, pp. 1665-69.
5. M. Azrin and W.A. Backofen: *Metall. Trans.*, 1970, vol. 1, pp. 2857-65.
6. Z. Marciniak and K. Kuczynski: *Int. J. Mech. Sci.*, 1967, vol. 9, pp. 609-20.
7. A.K. Tadros and P.B. Mellor: *Int. J. Mech. Sci.*, 1978, vol. 20, pp. 121-34.
8. J. Gronostajski and A. Dolny: *Les Mem. Sci. Rev. Metall.*, 1980, vol. 77 (4), pp. 570-78.
9. S.P. Keeler: *Advances in Deformation Processing*, 21st Sagamore Conf., Plenum Press, New York, NY, 1974, pp. 127-57.
10. A.P. Lee and J.R. Hiam: *Sheet Met. Ind.*, 1978, vol. 55, pp. 631-41.
11. S.P. Keeler and W.G. Brazier: *Microalloying-75*, New York, NY, 1977, pp. 517-30.
12. J.W. Hutchinson, K.W. Neale, and A. Needleman: *Mechanics of Sheet Metal Forming*, Plenum Press, New York, NY, 1978, pp. 111-26.
13. U.S. Rao and R.C. Chaturvedi: *Proc. 13th Biennial Congr. of the IDDRG*, Melbourne, Australia, 1984, pp. 85-91.
14. M. Gotoh, J. Satoh, and K. Tanaka: *J. Jpn. Soc. Plast.*, 1986, vol. 27, pp. 268-72.
15. J.H. Schmitt and J.M. Jalinier: *Acta Metall.*, 1982, vol. 30, pp. 1799-1809.
16. T.B. Stoughton: *Computer Modeling of Sheet Metal Forming Process: Theory, Verification and Application*, TMS, Warrendale, PA, 1985, pp. 143-59.
17. N. Triantafyllidis and S.K. Samanta: *Proc. R. Soc. London A*, 1986, vol. 406, pp. 205-26.
18. N. Triantafyllidis: *Proc. Int. Symp. on Plastic Instability*, Presses de l'Ecole Nationale des Points et Chaussees, Paris, 1985, pp. 115-24.
19. W.F. Hosford: University of Michigan, Dept. of Materials, Science and Engineering, personal communication, 1992.
20. Z. Marciniak, K. Kuczynski, and T. Pokora: *Int. J. Mech. Sci.*, 1973, vol. 15, pp. 789-805.
21. R. Hill: *Proc. R. Soc. London A*, 1948, vol. 193, pp. 281-97.
22. W.F. Hosford: *Proc. 7th North American Metalworking Conf.*, Society of Manufacturing Engineers, Dearborn, MI, pp. 191-97.
23. A. Graf and W.F. Hosford: *Forming Limit Diagrams: Concepts, Methods and Applications*, TMS, Warrendale, PA, 1989, pp. 153-66.
24. K.S. Raghavan: *Interstitial-Free Steels: Processing, Fabrication and Properties*, Canadian Institute of Mining and Metallurgy, Ottawa, ON, Canada, 1991, pp. 175-94.
25. A.K. Ghosh and S.S. Hecker: *Metall. Trans. A*, 1974, vol. 5A, pp. 2161-64.
26. A. Barata da Rocha: *Forming Limit Diagrams: Concepts, Methods and Applications*, TMS, Warrendale, PA, 1989, pp. 183-202.